Theoretical study of short and long-term behavior in hollow core concrete slabs prestressed with FRP tendons

Pablo M. Páez Gus[1]

[1]*Instituto de Estructuras y Transporte, Facultad de Ingeniería, Universidad de la República*
Julio Herrera y Reissing 565, Montevideo, Uruguay
ppaez@fing.edu.uy

Abstract. The aim of this work is to assess the suitability of the use of fiber-reinforced polymer (FRP) tendons in simply supported, prestressed, hollow core slabs without concrete topping, with respect to their short and long-term behavior under service load conditions. In this research, the use of carbon fiber reinforced polymer (CFRP) and aramid fiber reinforced polymer (AFRP) tendons are examined. In the first part of this paper, we present a framework for the short and long-term analysis of prestressed, concrete, hollow core slabs with FRP tendons in the cracked and uncracked states. Then, based on a theoretical study, we compare the behavior of fully and partially prestressed, hollow core slabs with either FRP tendons or steel tendons. Our main conclusions are that hollow core slabs which have been prestressed with either CFRP or ARFP tendons show lower prestress losses and lower long-term deflections in the uncracked state and for the same initial prestressing stress levels Although insignificant differences were observed in the cracked state, the main advantage lies in better use of both materials (concrete and FRP tendons), as these can give better performance than prestressing with steel tendons.

Keywords: Fiber reinforced polymers; Hollow core slabs; Long-term; Serviceability; Prestressed concrete.

1 Introduction

Precast, prestressed, hollow core slabs are widely used in floor and deck systems in buildings, parking structures and even as slab decks in the construction of bridges. Compared to concrete beams, they are characterized by relatively high span-to-depth ratios, low reinforcement ratios and the absence of shear reinforcement. Depending on the environmental exposure conditions, prestressed concrete structures with steel tendons must be designed so that they do not undergo cracking under long-term loads. Creep and shrinkage of the concrete and relaxation of the prestressing tendons cause redistribution of the forces between the tendons and the concrete, resulting in a decrease in the prestressing force and an increase in long-term deflections. Although the flexural rigidity of cracked sections is lower than for uncracked ones, this effect is less pronounced in prestressed concrete structures than in reinforced ones. However, long-term deflections are higher in uncracked, prestressed concrete structures. The two main characteristics of FRP tendons that make them more attractive than steel tendons are their high tensile strength and a lack of corrosion. In this research, the use of carbon fiber reinforced polymer (CFRP) and aramid fiber reinforced polymer (AFRP) tendons are examined. Some analytical and experimental studies on the short and long-term behavior at service load of prestressed concrete beams with FRP tendons have been carried out by [1-4]. Matthys and Taerwe [5] have studied the behavior of prestressed concrete slabs with AFRP and steel tendons in a cracked state. They found that the long-term deflections of the slab were similar, being slightly higher for the slab with AFRP bars.

In the first part of this paper, we present a framework for the short and long-term analysis of prestressed, concrete, hollow core slabs with FRP tendons in the cracked and uncracked states. Then, based on a theoretical study, we compare the behavior of fully and partially prestressed, hollow, core slabs with either FRP tendons or steel tendons.

2 Material properties

2.1 FRP and steel tendons

Both carbon and aramid fiber tendons show linear elastic stress-strain behavior up to failure. FRP tendons, as well as steel tendons, experience some degree of relaxation when subjected to constant deformations maintained over time. CFRP tendons present a negligible relaxation, estimated at 1% at 1000 hours of loading and less than 3% at 50 years of loading, for stresses of the order of 60% of the guaranteed tensile strength. AFRP tendons present a relaxation of the order of 7% at 1000 hours of loading and of the order of 12.7% at 50 years of loading, for stresses of the order of 60% of the guaranteed tensile strength. Both of these cases are under normal exposure conditions, room temperature and humidity conditions [6-8]. For steel tendons, linear elastic behavior can be assumed up to the characteristic yield stress, and for low relaxation tendons this is of the order of 2.5% at 1000 hours of loading for stress levels of 70% of the characteristic tensile strength [9].

The short and long-term stress-strain relationship for the prestressed tendons (fiber or steel) can be written as follows, Eq. (1):

$$\sigma_{r(i)}(t) = E_{r(i)}\left(\varepsilon_{r(i)}(t) + \varepsilon_{r(i),0} - \varepsilon_{r,rel(i)}(t)\right) \tag{1}$$

where $E_{r(i)}$ and $\varepsilon_{r(i)}(t)$ are the elastic modulus and the strain of the tendon located at the i-th layer at time t, respectively, $\varepsilon_{r(i),0}$ and $\varepsilon_{r,rel(i)}(t)$ are the initial strain and strain due to relaxation (reduced relaxation) at time t. In the case of hollow core slabs, the number of prestressing layers is less than or equal to two.

2.2 Concrete

For flexural elements under short-term loads, the stress-strain relationship for the concrete can be expressed as Eq. (2) [9]:

$$\varepsilon_e = {}^{\sigma_c}/_{E_c} \text{ para} - 0{,}40 \cdot f_{cm} \leq \sigma_c \leq f_{ctm,fl} \tag{2}$$

where E_c is the modulus of elasticity of the concrete, σ_c is the stress, f_{cm} and $f_{ctm,fl}$ are the mean compressive strength and the flexural tensile strength for the concrete, respectively. In addition, concrete under environmental exposure conditions experiences shrinkage and creep (if subjected to loads held constant over time). The total strain of the concrete fiber at time t, can be expressed as in Eq. (3) [10]:

$$\varepsilon(t) = \frac{(1+\phi(t,t_0))}{E_c(t_0)}\sigma_c(t_0) + \frac{1+\chi(t,t_0)\phi(t,t_0)}{E_c(t_0)}\Delta\sigma_c(t) + \varepsilon_{sh}(t,t_s) \tag{3}$$

where $\chi(t,t_0)$ is the aging coefficient, $\phi(t,t_0)$ is the creep coefficient between times t_0 and t, $E_c(t_0)$ is the modulus of elasticity of the concrete at time t_0 and $\varepsilon_{sh}(t,t_s)$ is the shrinkage strain between times t_s and t.

3 Framework for the short- and long-term analysis

The theoretical development and analysis of hollow core slabs presented in this work is based on the Navier-Bernoulli assumptions and it is assumed to be valid for both cracked and uncracked sections. A perfect bond between the concrete and prestressing tendons is also assumed, whether they are made of steel or FRP. Concrete can be considered as an aging, linear, viscoelastic material.

3.1 Initial prestressing force

In the design of prestressed concrete elements, the initial prestressing force is conditioned by the stress that the tendons are able to withstand and by the service conditions that the concrete must meet. In the case of steel tendons, the prestressing force is limited to the lowest value between 75% of the ultimate tensile strength and 85% of the characteristic yield strength f_{pk}. In the case of FRP tendons, the prestressing force is limited by the creep-rupture strength. When prestressing tendons are subjected to a constant stress over time, they experience creep,

that is, they deform over time at constant stress. If the initial stress is greater than a certain value, called the creep-rupture strength, the specimen reaches a third stage of creep for which the sudden rupture of the tendon occurs due to excessive deformation [11]. For Arapree tendons, studies have shown that the creep-rupture strength is of the order of 52% of the guaranteed tensile strength [12]. Creep depends on the environmental exposure conditions, such as temperature, humidity and attack by chemical substances (alkaline, acidic, saline exposure, etc.) [6, 7]. The creep-rupture strength for CFRP tendons is of the order of 79% of the guaranteed tensile strength [8].

3.2 Transfer length

Another important aspect to take into account in the analysis of prestressed concrete elements is the transfer length. The transfer length is the length of tendon necessary to transfer the prestressing force to the concrete. Therefore, prestressing force is not constant along the element. Zou [8] proposed that, for the transfer length l_t the expression is given by Eq. (4):

$$l_t = \frac{\mathrm{K}}{\sqrt{f_{ck,j}}} D_N \tag{4}$$

where K is 480 (for indented CFRP Leadline tendons) or 240 (for AFRP Arapree tendons), $f_{ck,j}$ is the characteristic value of the cylinder compressive strength of the concrete at time j and D_N is the nominal diameter of the tendon.

In the case of Tokyo Rope CCFC tendons, transfer length can be calculated according to Eq. (5) [13]:

$$l_t = \frac{f_{pi}}{\mathrm{K}\, f_{ck,j}^{0.67}} D_N \tag{5}$$

where f_{pi} is the initial prestressing stress of the tendon and K is 4.8 for CCFC tendons.

In the case of steel tendons, in this work the guidelines of the UNE-EN 1992-1-1 were followed [14].

3.3 Contribution of concrete between cracks

When, in a section of a member subjected to bending, the tensile stress in the concrete exceeds its flexural tensile strength, the section cracks. Although concrete is not able to carry much tensile force at the section, the intact concrete between cracks carries considerable tensile force. This contribution of the concrete between cracks is called 'tension stiffening'. When a concrete element is subjected to a combination of axial force and bending moment, the mean axial strain and mean curvature can be obtained from Eq. (6) [15]:

$$\varepsilon_m = (1-\zeta)\varepsilon_{O,1} + \zeta\varepsilon_{O,2} \tag{6a}$$

$$\kappa_m = (1-\zeta)\kappa_1 + \zeta\kappa_2 \tag{6b}$$

$\varepsilon_{O,1}$ and $\varepsilon_{O,2}$ are the axial strain at the reference point O for the applied load, assuming an uncracked and cracked state for the section, respectively; κ_1 and κ_2 are the curvature of the section assuming uncracked and cracked state, respectively; and ζ is a dimensionless coefficient whose expression is given by Eq. (7) [14, 15]:

$$\zeta = 1 - \beta\left(\frac{f_{ctm}}{\sigma_{1,\max}}\right)^2 \tag{7}$$

where β is the load duration factor and $\sigma_{1,\max}$ is the value of the tensile stress at the extreme fiber of the section assuming no cracking. According to Bischoff [17], this expression can be applied to both steel and FRP reinforced concrete elements since it is based on principles related to tension stiffening rather than empirical ones.

3.4 Short- and long-term cross sectional analyses at service loads

According to Eq. (6), the calculation of the mean axial strain of a concrete fiber of the section requires two analyses, one considering cracking and the other without. If we consider a hollow core slab and Oyz is the system of referencing the axes, such that the vertical axis Oz is positive downwards (belonging to the axis of symmetry) and the reference point O is in the upper fiber. In the typical constructive sequence of these types of elements, the loads are applied at different ages, where t_0 is the time of the prestressing transfer and t_i is any time after t_0 for which a load is applied. The analysis when the section is not cracked is quite straightforward. At time of transfer,

the axial strain at *O* and the curvature are expressed as Eq. (8):

$$\begin{bmatrix}\varepsilon_O(t_0)\\ \kappa(t_0)\end{bmatrix} = \hat{R}(t_0)\cdot\begin{bmatrix}N_{ext}(t_0)-\sum_{i=1}^{i=m_p}E_{r(i)}\varepsilon_{r(i),0}A_{r(i)}\\ M_{ext}(t_0)-\sum_{i=1}^{i=m_p}E_{r(i)}\varepsilon_{r(i),0}A_{r(i)}z_{r(i)}\end{bmatrix} \tag{8}$$

where $N_{ext}(t_0)$ and $M_{ext}(t_0)$ are the axial force at *O* and the bending moment at time t_0, respectively. $\hat{R}(t_0)$ is the flexibility matrix of the section and is given by Eq. (9):

$$\hat{R}(t_0) = \left(\frac{1}{(R_A(t_0)R_I(t_0)-R_B(t_0)^2)}\right)\cdot\begin{bmatrix}R_I(t_0) & -R_B(t_0)\\ -R_B(t_0) & R_A(t_0)\end{bmatrix} \tag{9}$$

where $R_A(t_0)$, $R_B(t_0)$ and $R_I(t_0)$ are the axial rigidity, the rigidity related to the first order moment of area and the flexural rigidity of the transformed cross-section, with respect to the reference axes at time t_0, respectively. The axial stain at *O* and the curvature due to any other external load applied at any time t_i can be obtained analogously by means of Eq. (5) without including the prestressing term. The variation in the axial strain at *O* and the curvature between times t_{j-1} and t_j can be obtained by Eq. (10):

$$\begin{bmatrix}\Delta\varepsilon_r(t_j)\\ \Delta\kappa(t_j)\end{bmatrix} = \hat{R}(t_j)\cdot\left(E_{c,TB}(t_j)\sum_{i=0}^{i=j-1}\hat{F}_e(t_j,t_i)\begin{bmatrix}N_c(t_i)\\ M_c(t_i)\end{bmatrix} + E_{c,TB}(t_j)\varepsilon_{sh}(t_j,t_0)\begin{bmatrix}A_c\\ B_c\end{bmatrix} + \sum_{i=1}^{i=m_p}A_{r(i)}E_{r(i)}\varepsilon_{r,rel(i)}(t_j)\begin{bmatrix}1\\ z_{r(i)}\end{bmatrix}\right) \tag{10}$$

where $\hat{R}(t_j)$ is the flexibility matrix of the transformed cross-section using $E_{c,TB}$, $E_{c,TB}$ being the age-adjusted effective modulus ($E_{c,TB}=(1+\chi(t_j,t_{j-1})\phi(t_j,t_{j-1}))/E_c(t_{j-1})$), $z_{r(i)}$ is the position of the *i*-th tendon layer, N_c and M_c are the axial force at *O* and the bending moment of the concrete due to the load applied at time t_i, A_c and B_c are the area and the first order moment of area of the concrete with respect to *Oy*-axes, respectively. $\hat{F}_e(t_j,t_i)$ is given by Eq. (11):

$$\hat{F}_e(t_j,t_i) = \frac{\phi(t_j,t_i)-\phi(t_{j-1},t_i)}{E_c(t_i)} \tag{11}$$

If, under the action of an external axial force and a bending moment applied at time t_i, $N_{ext}(t_i)$, $M_{ext}(t_i)$, and $f_{ctm,fl}$ are reached in some fibers, assuming an uncracked section, then the section cracks. In this case, the analysis is somewhat more complex, although the principle of superposition is valid for the linear viscoelastic material, the sectional analysis is non-linear. $N_{ext}(t_i)$ and $M_{ext}(t_i)$ can partition into two components, Eq. (12):

$$\begin{bmatrix}N_{ext}(t_i)\\ M_{ext}(t_i)\end{bmatrix} = \begin{bmatrix}N_1(t_i)\\ M_1(t_i)\end{bmatrix} + \begin{bmatrix}N_2(t_i)\\ M_2(t_i)\end{bmatrix} \tag{12}$$

where $N_1(t_i)$ and $M_1(t_i)$ are the internal forces necessary to bring the existing stress in the concrete just before the application of $N_{ext}(t_i)$ and $M_{ext}(t_i)$ to zero, and $N_2(t_i)$ and $M_2(t_i)$ are the forces that produce cracking. Under the action of the internal forces $N_2(t_i)$ and $M_2(t_i)$, it is necessary to carry out an iterative procedure to obtain the neutral axis depth. The time-dependent analysis is carried out by applying Eq. (10), assuming that the neutral axis depth does not vary with time, resulting in small errors [17]. Cross-sectional properties are calculated for the cracked section and A_c and B_c are the area and the first order moment of area of the concrete with respect to *Oy* of the uncracked concrete part, respectively.

3.5 Deflection calculation and computational implementation

In order to carry out the proposed analysis, a computational algorithm was implemented. The span of the hollow core slab is divided into a number of sections for which the described formulation is applied. Deflection is calculated by double numerical integration of the curvature from the mean curvature.

4 Case study

For the purposes of this study, a typical section of a hollow core slab was considered, the geometry of which is shown in Fig. 1. The slab was simply supported with a span length of 8.0 m, the characteristic compressive cylinder strength of the normal Portland cement concrete was 35 MPa, relative humidity was 70% and ambient

temperature 20ºC. Wet curing was assumed during the first three days, at which time the prestressing is transferred. Five types of slabs were designated, depending on the manufacturer and the arrangement of tendons used, according to Tables 1 and 2, with the main characteristic that the initial prestressing force is the same for all of them.

Three load cases were considered in this study. In the first, it was assumed that the only long-term load (excluding prestressing) was the self-weight of the slab, q_W=3.49 kN/m. In the second, it was assumed that, in addition to the self-weight, a dead load q_{DL} of 5.80 kN/m was applied at 28 days of age and kept constant until 10000 days. Under this load the slab does not crack. In the third case, under the same considerations as the previous one, the load q_{DL} was considered to be 9.75 kN/m, in this case the slab cracked.

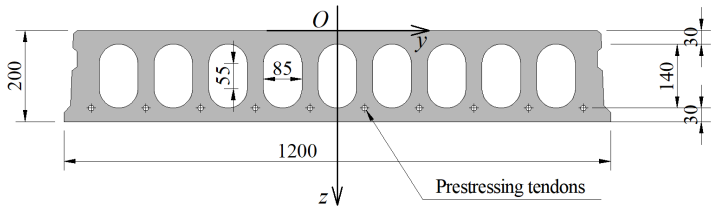

Figure 1. Cross section of the concrete hollow core slab.

Table 1. Hollow core slabs designations and prestressing properties.

Hollow core designation	Tendon manufacturer	Tendon designation	Tensile modulus [GPa]	Capacity [MPa]	Tendon section [mm^2]	Allowable initial stress
HC-C1	Tokyo Rope	1x7-Φ10.5	155	2439	57.8	0.6×f_{pu} (*)
HC-C2	Carbopree	Φ10	130	2450	78	0.6×f_{pu} (*)
HC-A	Arapree	Φ12	61	1400	114	0.4×f_{pu} (*)
HC-S1	Acindar	1x7- Φ12.7	195	1860	98.7	0.75×f_{pu} (**)
HC-S2	Acindar	1x7- Φ12.7	195	1860	98.7	0.75×f_{pu} (**)

(*) Based on ACI 440.4 recommendations [18].

Table 2. Hollow core slabs designations and prestressing properties, continued.

Hollow core designation	Number of tendons	Allowable initial force per tendon [N]	Initial force per tendon [N]	Initial prestressing force [N]	Initial stress [MPa]
HC-C1	9	84585	70933	638397	1227 (0.46× f_{pu})
HC-C2	7	114660	91200	638400	1169 (0.48× f_{pu})
HC-A	10	63740	63840	638400	560 (0.4× f_{pu})
HC-S1	7	91791	91200	638400	924 (0.50× f_{pu})
HC-S2	5	137687	127680	638400	1294 (0.70× f_{pu})

4.1 Analysis, comparison and discussion of the results

Figure 2 shows the midspan deflection and prestress loss in the same section as a function of time for each of the designations used. The numbers 1 and 2 (followed by the designation) refer to load Case Nº1 (black) and Nº2 (red), respectively. Regarding load Case Nº1 (self-weight and prestressing), the lowest long-term deflection of the slab is obtained for steel tendons, this being of the order of 20 mm upwards, and it is of the order of 25% higher for FRP tendons. Regarding the prestress loss, the greatest losses are also obtained for steel tendons, this being of the order of 22% for the HC-S2 case. This can be explained, among other factors, by the high initial stress which causes a greater loss by relaxation of the steel. On the other hand, the least loss is obtained in the case of

CFRP tendons.

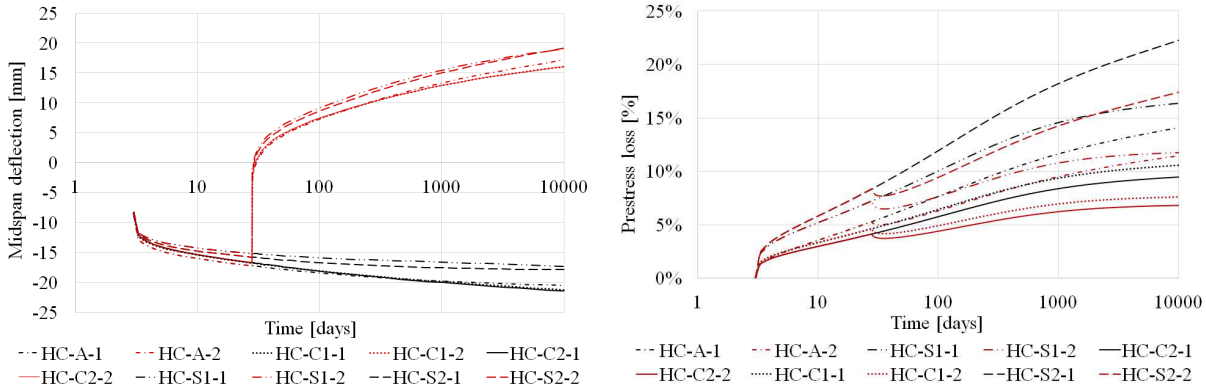

Figure 2. Midspan deflection and prestress loss. Numbers one and two follow the hollow core designations in the loads for Case Nº1 and Case Nº2, respectively.

With respect to load Case Nº2, the maximum midspan deflections are obtained for the steel tendons, these being downwards and of the order of 19 mm. The smallest midspan deflection is obtained with the use of CFRP tendons and is of the order of 16 mm, which represents 16% less than those of steel. With AFRP tendons the midspan deflection is of the order of 17 mm. Similar to the previous case, prestress losses are greater for steel tendons. This behavior for uncracked sections can be explained as follows. Since all slabs are subjected to the same initial stress level (or approximately the same) and the same environmental exposure conditions, the unrestrained strain of the concrete at the level of the center of gravity of the tendons is approximately the same (except for HC-A and HC-S2, which are somewhat higher due to the relaxation of the tendons). On the other hand, since the section is uncracked, the properties of the transformed cross-section by the age-adjusted effective modulus do not differ significantly from each other. Therefore, the variation of the strain at the level of the center of gravity of the tendons is approximately the same for all the slabs and, due to the lower modulus of elasticity of the FRP tendons, this translates into a lower loss of prestress.

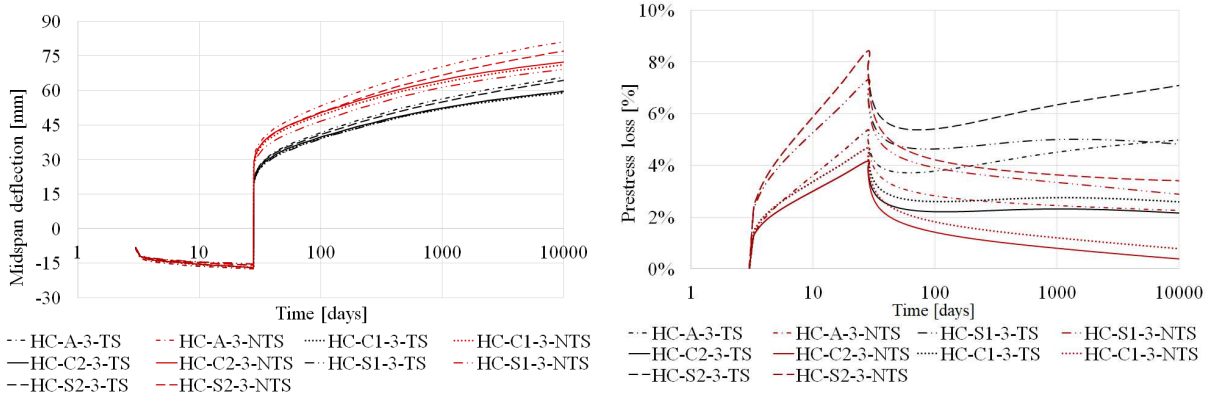

Figure 3. Midspan deflection and prestress loss. Number three follows the hollow core designation referring to Case Nº3 and TS and NTS refers to whether the tension stiffening effect was considered or not, respectively.

Figure 3 shows the midspan deflection and the prestress loss as a function of time for load Case Nº3. The initials NT and NTS (followed by the number) indicate whether or not the contribution of the concrete between cracks has been considered, respectively. It is important to note that the beneficial effect of considering the contribution of concrete between cracks, being the total midspan deflection at 10000 days for the case of AFRP tendons, is approximately 19% lower due to this effect. On the other hand, the highest total mid-span deflections were obtained for the HC-A (AFRP tendons) and HC-S2 (steel tendons) slabs. The first one can be explained by the very low modulus of elasticity exhibited by AFRP tendons; in other words, the stiffness of the transformed, cracked, cross-section from the ratio of modulus of elasticity between the tendons and the concrete is lower. Although for the HC-S2 slab, the stiffness of the transformed cracked cross-section is much higher, the greater

total mid-span deflection can be explained by the high prestress loss which translates into greater downward deflections. If tension stiffening is taken into account, the HC-C1, HC-C2 and HC-S1 slabs present very insignificant differences in relation to the total mid-span deflection, this being of the order of 60 mm.

5 Conclusions

Hollow core slabs, prestressed with either CFRP or ARFP tendons, show lower prestress losses than those prestressed with steel tendons in both cracked and uncracked states and for the same initial prestressing stress levels. For slabs in the uncracked state and under loads that produce camber, the long-term deflections in slabs prestressed with FRP tendons are greater than those prestressed with steel tendons (in absolute value terms). However, under loads that produce sagging, long-term deflections in slabs prestressed with FRP tendons are smaller. On the other hand, if the contribution of concrete between cracks is considered, insignificant differences are observed in the long-term deflection in the cracked state. Therefore, it is possible to conclude that the main advantage lies in better use of the concrete and the FRP tendons, as these can give better performance than prestressing with steel tendons.

Authorship statement. The author hereby confirm that he is the sole liable person responsible for the authorship of this work, and that all material that has been herein included as part of the present paper is either the property (and authorship) of the author, or has the permission of the owners to be included here.

References

[1] A. Braimah, M. F. Green and K. A. Soudki, "Long-term behavior of CFRP prestressed concrete beams". *PCI Journal*, vol. 48, n. 2, pp. 98-107, March-April 2003.

[2] P. X. W. Zou, "Theoretical study on short-term and long-term deflection of fiber reinforced polymer prestressed concrete beams". *ASCE Journal of Composites for Construction*, vol. 7, n. 4, pp. 285–91, 2003.

[3] P. X. W. Zou and S. Shang, "Time-dependent behaviour of concrete beams pretensioned by carbon fibre-reinforced polymers (CFRP) tendons", *Construction and Building Materials*, vol. 21, pp.777-88, 2007.

[4] S. A. Youakim and V. M. Karbhari, "An approach to determine long-term behavior of concrete members prestressed with FRP tendons", *Construction and Building Materials*, vol. 21, pp.1052-60, 2007.

[5] S. Mathys and L. Taerwe, "Long-term behaviour of concrete slabs pretensioned with AFRP or prestressing Steel", *Durability of Fibre Reinforced Polymer (FRP) Composites for Construction*, pp. 95-106, 1998.

[6] H. Saadatmanesh and F. E. Tannous, "Long-term behavior of aramid fiber reinforced plastic (AFRP) tendons". *ACI Materials Journal*, vol. 96, n. 3, pp. 297-305, May-June 1999.

[7] H. Saadatmanesh and F.E. Tannous, "Relaxation, creep, and fatigue behavior of carbon fiber reinforced plastic tendons", *ACI Materials Journal*, vol. 96, n. 2, pp. 143–153, 1999.

[8] P.X.W. Zou, "Long-term properties and transfer length of fiber-reinforced polymers", *Journal of Composite for Construction,* vol. 7, n. 1, pp. 10–19, 2003.

[9] International Federation for Structural Concrete (FIB). Model Code 2010, vol. 1. CEB-FIP Bulletin no. 65. *Federation Internationale du Béton*, Lausanne, Switzerland, 2012.

[10] Z. P. Bazant, "Prediction of concrete creep effects using age-adjusted effective modulus method", ACI Journal, vol. 69, pp. 212–7, 1972.

[11] G.B. Guimaraes and C.J. Burgoyne, "Creep behaviour of a parallel-lay aramid rope", *Journal of Materials Science*, vol. 27, pp. 2473–89, 1992.

[12] A. Gerritse and J. A. Den Uijl, ''Long-term behaviour of Arapree.'' *Proceeding of the 2nd International Symposium on Non-Metallic (FRP) Reinforcement for Concrete Structures*, London, pp. 57–66, 1995.

[13] Z. I. Mahmoud, S. H. Rizkalla and E. E. R. Zaghloul, "Transfer and Development Length of CFRP Reinforcement," *Proceedings of 1997 CSCE Annual Conference*, pp. 101-110, 1997.

[14] UNE-EN 1992-1-1:2013/A1:2015, Eurocode 2: Design of concrete structures – Part 1-1: General rules and rules for buildings, 2016.

[15] A. Ghali, R. Favre and M. Eldbadry, *Concrete structures: stresses and deformation*. 3rd ed. New York, Spon Press, 2002.

[16] P. H. Bischoff, "Reevaluation of deflection prediction for concrete beams reinforced with steel and fiber reinforced polymer bars", *ASCE Journal of Structural Engineering*, v. 131, n. 5, pp. 752-67, 2005.

[17] R. I. Gilbert and G. Ranzi, *Time-dependent behaviour of concrete structures*. New York, Spon Press, 2011.

[18] ACI Committee 440.4R-04. Prestressing concrete structures with FRP tendons. American Concrete Institute. Farmington Hills, MI, 2004.